Nonhydrostatic Atmospheric Modeling using a *z*-Coordinate Representation

JÜRGEN STEPPELER

Deutscher Wetterdienst, Offenbach, Germany

HEINZ-WERNER BITZER

AWGeophys–OrgELBW, Offenbach, Germany

MAUD MINOTTE

University of Bonn, Bonn, Germany

LUCA BONAVENTURA

Dipartimento di Ingegneria Civile ed Ambientale, Università degli Studi di Trento, Trento, Italy

4 June 2001 and 13 February 2002

ABSTRACT

A representation of the orography based on approximate finite-volume techniques is applied to a nonhydrostatic atmospheric model. Techniques previously developed by the authors in the context of a semi-implicit, semi-Lagrangian model are applied also to a Eulerian, split-explicit model. Furthermore, an improved formulation of the original approach is introduced, which allows for better orography representation by introducing a simplified version of the most general shaved cells. A two-dimensional numerical test shows that the method developed does not suffer from the problems reported in connection with the η-coordinate.

1. Introduction

Numerical models for operational weather prediction will be able to use grids between 1 and 10 km within the next few years. This development requires the use of nonhydrostatic models. The purpose of such finescale models will be to predict the local weather, including elevated fog, produced by stratiform clouds touching mountains. Nonhydrostatic models using terrain following coordinates, such as the Pennsylvania State University–National Center for Atmospheric Research (Penn State–NCAR) fifth-generation Mesoscale Model (MM5; Dudhia 1993) or the Lokal-Modell (LM; Steppeler et al. 2002) are not well suited for such predictions. Numerical errors can be induced around steep slopes, where the Jacobian of the coordinate transformation is almost singular. The stratified atmosphere generates artificial forces, caused by numerical errors. These can produce artificial circulations that destroy clouds in the vicinity of mountains. For example, in the model LM, the condition that such numerical forces remain reasonably small is $\delta h < dz$, with δz being the layer thickness and δh the change of orography between one grid point and the next. This condition is violated in most operational models, even for larger-scale operational hydrostatic applications. With fine meshes, the model orography tends to be steeper than for coarser meshes. Therefore the circulations driven by numerical errors can be substantial (Sundqvist 1976). For models using the terrain-following coordinate, such as MM5 or LM, a spatially homogeneous reference profile is introduced, in order to reduce this effect. If this reference profile is close to the real state of the atmosphere in the model, the error mentioned is absent, and nearly perfect simulations of gravitational waves can be done. This is the situation investigated in this paper. As in addition rather smooth grid representations of the mountain are used, the terrain-following coordinate can be supposed to simulate these tests very well. For operational applications on large areas it will not be possible to choose a horizontally homogeneous atmospheric reference state in the way indicated. Therefore operational applications

Corresponding author address: Dr. Jürgen Steppeler, Deutscher Wetterdienst, Frankfurterstr. 135, 63067 Offenbach, Germany.
E-mail: juergen.steppeler@dwd.de

© 2002 American Meteorological Society

will always suffer from numerically generated artificial forces near mountains.

A method to reduce this error has been proposed by Mesinger et al. (1988). This method reduces the coordinate deformation by having the model layers not following the mountains, but rather ending at mountains. The lower boundary is treated under the assumption that it is represented by a step function. While this coordinate has the expected advantages in low wind situations, it has disadvantages concerning the flow around smooth topography. In particular, Gallus and Klemp (2000) reported a failure to produce proper mountain-induced gravitational waves. As opposed to this, the test case proposed by Gallus and Klemp (2000) is simulated properly using the terrain-following coordinate. Another *z*-coordinate approach was proposed by G. Tripoli (2001, personal communication). This approach was presented at the Third International Workshop on Nonhydrostatic Modelling in Offenbach, Germany, held in 1999, and does not suffer from the problems mentioned above. A short report on the workshop is given by Saito et al. (2001). The method used by Tripoli is based on posing lower boundary values for the velocity components using assumptions on the vorticity. In the present paper a different method is used to obtain the approximation near the lower boundary. The free-slip boundary condition is used and numerically evaluated using the finite-volume approximation.

With simple equations a sufficient convergence condition is met when the domain boundary is a continuous spline. Such a condition is present in the *z*-coordinate atmospheric model described here, being based on the shaved element method, used in computational fluid dynamics and oceanography (Adcroft et al. 1997). A Cartesian structured grid corresponding to the case without orography is assumed and the topography is assumed to be represented by a bilinear spline with nodes at the grid points with half values of the *x* axis. There are three types of grid squares: those that are completely under the earth, those completely above the topography, and those that are cut by the topography function. The first two classes of elements can be treated in an obvious way. The volumes that are cut by the orography are treated by the finite-volume method.

Without further approximations this method may require very small time steps, since the elements cut from a volume may be rather small. One solution would be to use a semi-implicit discretization (Thomas et al. 2000). Here we use the time-splitting method, as introduced by Klemp and Wilhelmson (1978). This has been shown by Saito et al. (1998) to have good operational efficiency with the LM. The problem of a restrictive Courant–Friedrichs–Lewy (CFL) criterion with small cutoff elements is solved by using the thin-wall approximation, which is common in oceanography. An atmospheric use of this method was tested by Bonaventura (2000). The derivation of this method from the shaved element approach requires, in addition to the vertical walls, the use of horizontal walls, which differs from the method proposed by Bonaventura (2000), which uses vertical walls only. Test integrations using this method in two space dimensions will be given in section 3. The test problems proposed by Gallus and Klemp (2000) are simulated properly by the *z*-coordinate version of LM.

2. Description of the *z*-coordinate LM

The treatment of the lower boundary in *z*-coordinates is based on the nonhydrostatic equations, as used for example in MM5 (Dudhia 1993) or LM (Steppeler et al. 2002). They are given here in *z*-coordinates:

$$\frac{\partial u}{\partial t} = -u\frac{\partial u}{\partial x} - w\frac{\partial u}{\partial z} - \frac{1}{\rho}\frac{\partial p}{\partial x} \tag{1}$$

$$\frac{\partial w}{\partial t} = -u\frac{\partial w}{\partial x} - w\frac{\partial w}{\partial z} - \frac{1}{\rho}\frac{\partial p}{\partial z} - g \tag{2}$$

$$\frac{\partial p}{\partial t} = -u\frac{\partial p'}{\partial x} - w\frac{\partial p'}{\partial z} + g\rho_0 w - \frac{C_p}{C_v}p\left(\frac{\partial u}{\partial x} + \frac{\partial w}{\partial z}\right) \tag{3}$$

$$\frac{\partial T}{\partial t} = -u\frac{\partial T}{\partial x} - w\frac{\partial T}{\partial z} - \frac{p}{\rho C_v}\left(\frac{\partial u}{\partial x} + \frac{\partial w}{\partial z}\right). \tag{4}$$

Because this paper focuses only on the principal usefulness of the method, the dry-adiabatic form of the nonhydrostatic equations of motion [Eqs. (1)–(4)] is used as in Dudhia (1993). The grid is shown in Fig. 1. At the center i, j of a cell, T and P are defined. The horizontal and vertical components of the velocity are defined at the boundaries of a cell for half levels of i or k. This is indicated for the cell $i, k + 1$ in Fig. 1. The orographic function is indicated by a heavy dark line. It is a linear continuous spline with node points at half values of i on the x axis. The finite-volume method leads to a spatial discretization. The amplitudes shown are representative of area averages over the cell, rather than being point values. The application of the finite-volume method is explained for the example of the approximation of the divergence of the field (U, W).

The discretization of the divergence term $D = \mathrm{div}(U, W)$ is done applying Stokes's theorem over the cell volume. It is assumed that D is represented by gridpoint values $D_{i,k}$ defined at the cell centers. The integration is performed under the assumption that $D_{i,k}$ is constant over a cell. An approximation of $D_{i,k}$ at the cell centers is obtained by assuming that the values of u and w are approximated by constants on the cell boundaries. Here, $dz'_{i-1/2,k}$ and $dz'_{i+1/2,k}$ are the parts of the boundaries of the cell i, k above the ground. Both dx' and dz' are shown in Fig. 1 for the sides of cell i, k. In this particular case the cell sides $i + 1/2, k$ and $i - 1/2, k$ are partly above the ground, making the corresponding dz' smaller

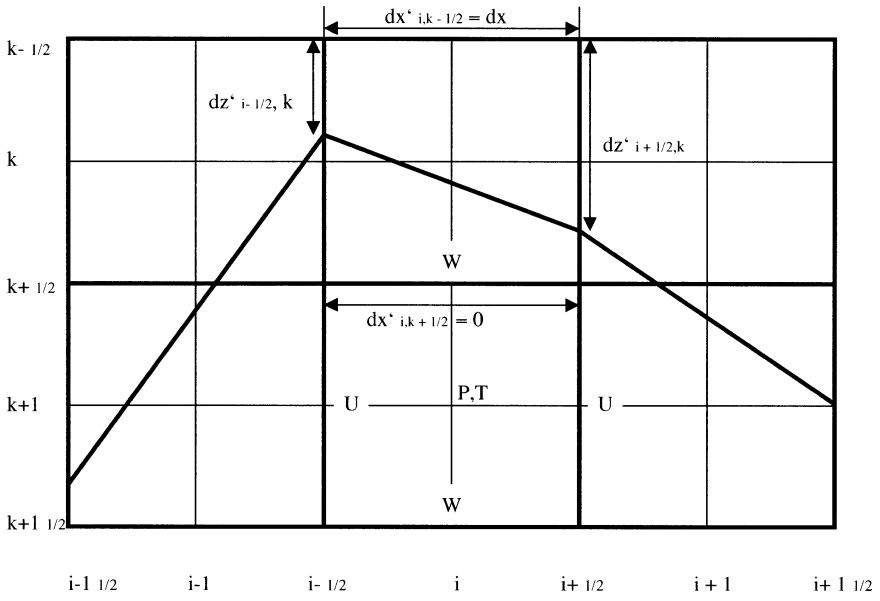

FIG. 1. The grid for the *z*-coordinate representation.

than the full cell sides. Also, $dx'_{i,k+1/2}$ is completely under the ground resulting in $dx'_{i,k+1/2} = 0$, and $dx'_{i,k-1/2}$ is completely above the ground, resulting in $dx'_{i,k-1/2} = dx$. For an orography other than that shown in Fig. 1, it may happen that the bottom cuts through a horizontal cell boundary, leading to $dx'_{i,k-1/2}$ equaling neither 0 nor dx. If the volume of the area cut off by the orography is $V_{i,k}$, we obtain the following equation for the gridpoint values of the divergence:

$$\begin{aligned} D_{i,k}V_{i,k} &= \int \left(\frac{\partial u}{\partial x} + \frac{\partial w}{\partial z}\right) dx\, dz \\ &= dx'_{i,k-1/2}w_{i,k-1/2} - dx'_{i,k+1/2}w_{i,k+1/2} \\ &\quad + dz'_{i+1/2,k}u_{i+1/2,k} - dz'_{i-1/2,k}u_{i-1/2,k}. \end{aligned} \tag{5}$$

If the orography is different from that shown in Fig. 1, and the whole cell is completely above the orography, we have $dx'_{i,k-1/2} = dx$ and $dz'_{i-1/2,k} = dz_k$. In this case the equation above describes the usual second-order centered-difference approximation to the divergence. For the shaved elements, the volumes can be rather small, which would lead to rather stringent CFL conditions. We use here the thin-wall approximation, consisting of the assumption

$$V_{i,k} = dxdz_k. \tag{6}$$

The index of dx is dropped, since we consider only the situation of a homogeneous horizontal resolution, when dx does not depend on i. Equation (6) means that $D_{i,k}$ is considered as a cell average over the whole cell, rather than the small cutoff element. The physical picture of this situation is that the cells are hollow and filled with air, as if the grid under the mountain consisted of infinitely thin walls, from which the mountains are cut out. A cut cell is open to the surrounding atmosphere. Bonaventura (2000) has used this approximation for two-dimensional atmospheric simulations. The derivation of this approximation from the finite-volume method used here implies in addition to the dz' the use of horizontal thin walls of lengths dx', which differs from the method of Bonaventura (2000), who uses vertical thin walls of length dz' only. For a mountain, which is so shallow that it is contained within the lowest layer, the approximation derived here is identical to that of Bonaventura (2000). For the advection terms Bonaventura uses the semi-Lagrangian method, which does not require specifying the lower boundary values. Here, we use finite-difference approximations for the advection terms. According to Gallus and Klemp (2000), different ways of posing the lower boundary condition have a rather essential impact on the realism of the simulated flow around the mountain. The approximations used here are again obtained by integrating over a computational cell under the assumption that the fields are represented by piecewise constant functions. According to Steppeler (1982) the derivatives of the piecewise constant functions are obtained using the theory of distributions. In the case where a divergence term is evaluated, the approximation given by Steppeler (1982) reduces to the common finite-volume approximation. Using again the thin-wall approximation, the advection in x direction of $q_{i,k}$ is approximated as

$$\begin{aligned} u\frac{\partial q}{\partial x_{i,k}} = \frac{1}{2}\Bigg[&\frac{u_{i-1/2,k}dz'_{i-1/2,k}(q_{i,k} - q_{i-1,k})}{dx} \\ &+ \frac{u_{i+1/2,k}dz'_{i+1/2,k}(q_{i+1,,k} - q_{i,k})}{dx}\Bigg]. \end{aligned} \tag{7}$$

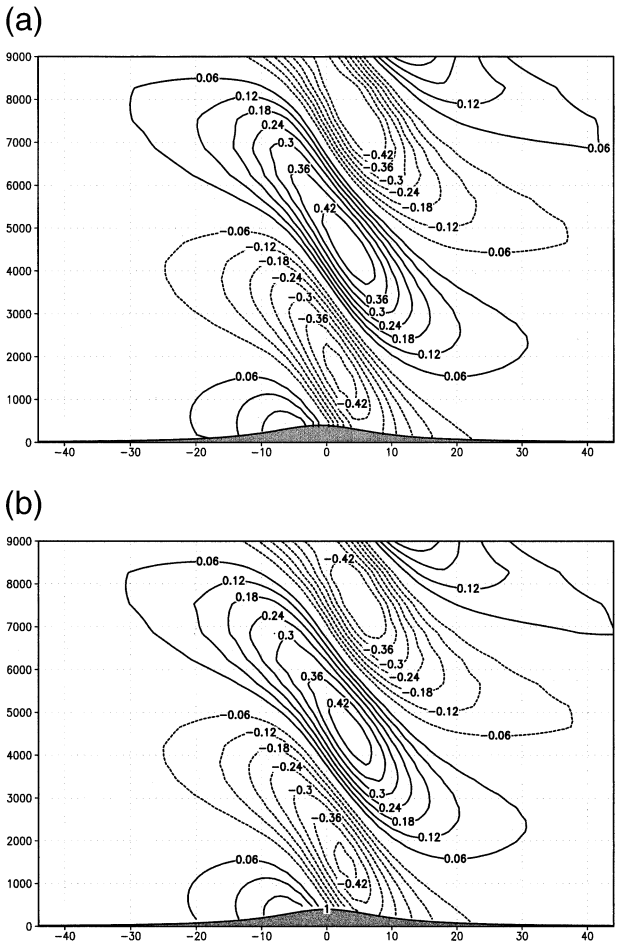

FIG. 2. Vertical velocity in m s^{-1} for the mountain of 400-m height; the vertical axis is marked in m and the horizontal in km. (a) Results obtained with the shaved-element method and (b) those of the terrain-following version of the model. The reference state was close to the state of the atmosphere as represented in the model, and the mountain was rather smooth. Therefore the terrain-following coordinate produces rather good results and both results are very similar.

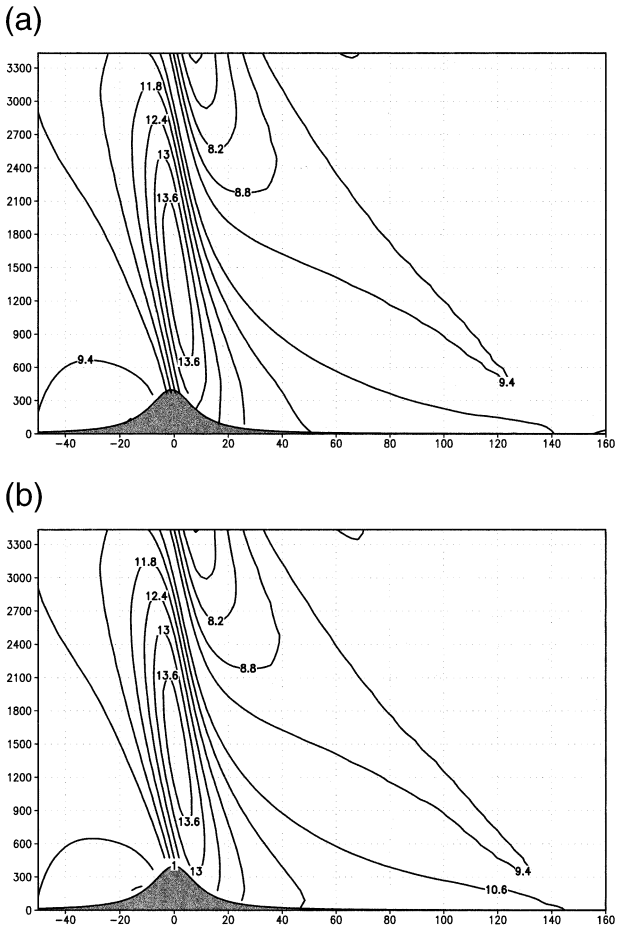

FIG. 3. As in Fig. 2 but for the horizontal velocity; note the different extent of the horizontal and vertical axes as compared to Fig. 2.

The approximation to Eqs. (1)–(4) can be formulated using flux limiters $F_{z,i+1/2,k}$ and $F_{x,i,k+1/2}$, defined as

$$F_{z,i+1/2,k} = dz'_{i+1/2,k}/dz_k \quad \text{and} \tag{8}$$

$$F_{x,i,k+1/2} = dx'_{i,k+1/2}/dx. \tag{9}$$

For the further description of the difference equations in z coordinates, the indices i and k will be dropped, if half or full levels are to be used. Only the spatial discretization will be described. The time discretization is done using the Klemp–Wilhelmson method (see Dudhia 1993; Steppeler et al. 2002). A C-grid representation is used, with p' and T being defined for i, k, u for $i + 1/2$, k and w for i, $k + 1/2$. The finite-difference equations approximating Eqs. (1)–(4) are formulated in terms of operators, which can be used with either half or full values of i and k, depending on the field ψ, they are applied to:

$$\overline{\psi}^{x} = (\psi_{i+1,k} + \psi_{i,k})/2 \tag{10}$$

$$\overline{\psi}^{z} = (\psi_{i,k+1} + \psi_{i,k})/2 \tag{11}$$

$$\delta_x\psi = (\psi_{i+1,k} - \psi_{i,k})/dx \tag{12}$$

$$\delta_z\psi = (\psi_{i,k+1} - \psi_{i,k})/dz_k; \quad \text{for } k = 1, 2, 3 \ldots \tag{13}$$

$$\delta_z\psi = (\psi_{i,k+1} - \psi_{i,k})/\overline{dz_k}^{z}; \quad \text{for } k = 1/2, 3/2, 5/2 \ldots \tag{14}$$

$$\frac{\partial u}{\partial t} = -\overline{\overline{F_z}^{x}\overline{u}^{x}\delta_x u}^{x} - \overline{\overline{F_x}^{x}\overline{w}^{x}\delta_z u}^{z} - \frac{1}{\overline{\rho}^{x}}\delta_x p \tag{15}$$

$$\frac{\partial w}{\partial t} = -\overline{\overline{F_z}^{z}\overline{u}^{z}\delta_x w}^{x} - \overline{\overline{F_x}^{z}\overline{w}^{z}\delta_z z}^{z} - \frac{1}{\overline{\rho}^{z}}\delta_z p - g \tag{16}$$

$$\frac{\partial p}{\partial t} = -\overline{F_z u\delta_x p'}^{x} - \overline{F_x w\delta_z p'}^{z} + g\rho_0 w - \frac{C_p}{C_v}D, \tag{17}$$

with D being an approximation of the divergence. Using the operators introduced above, the approximation of D introduced in Eq. (5) is written as

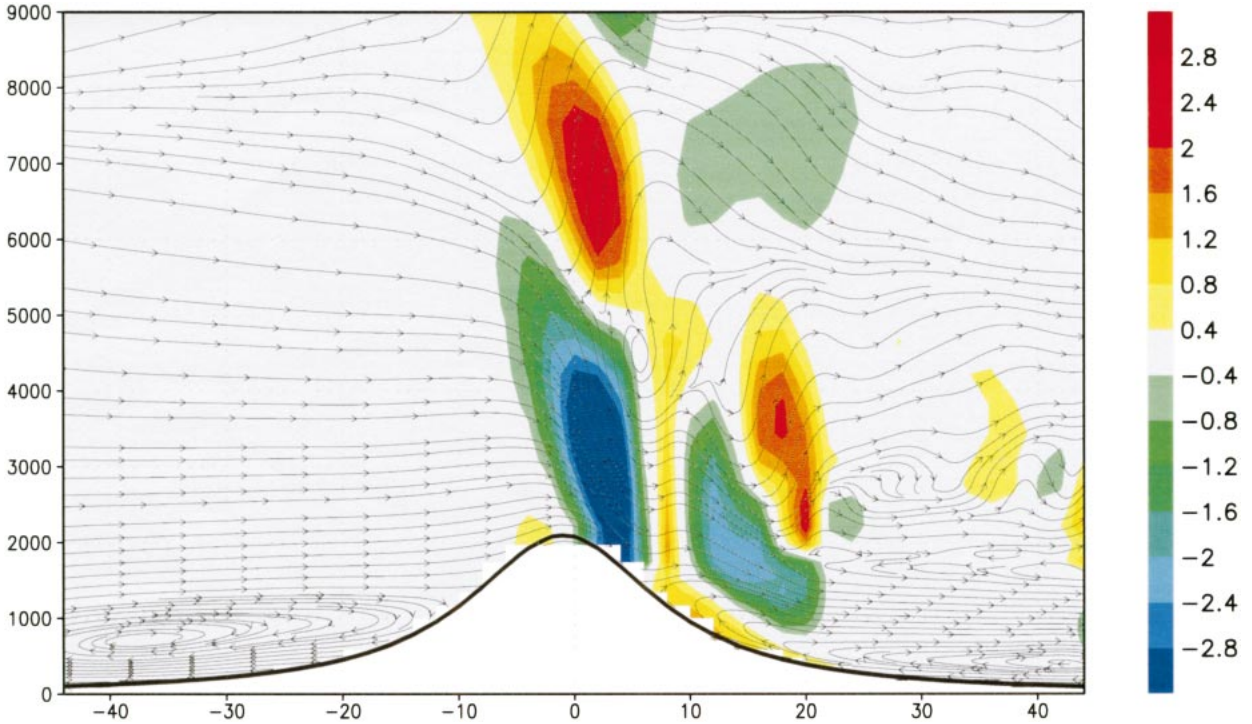

FIG. 4. Vertical velocity and streamlines for the flow behind a mountain of 2100-m height after 4 h. The vertical velocities are given in m s^{-1}. The vertical axis is marked in m and the horizontal in km.

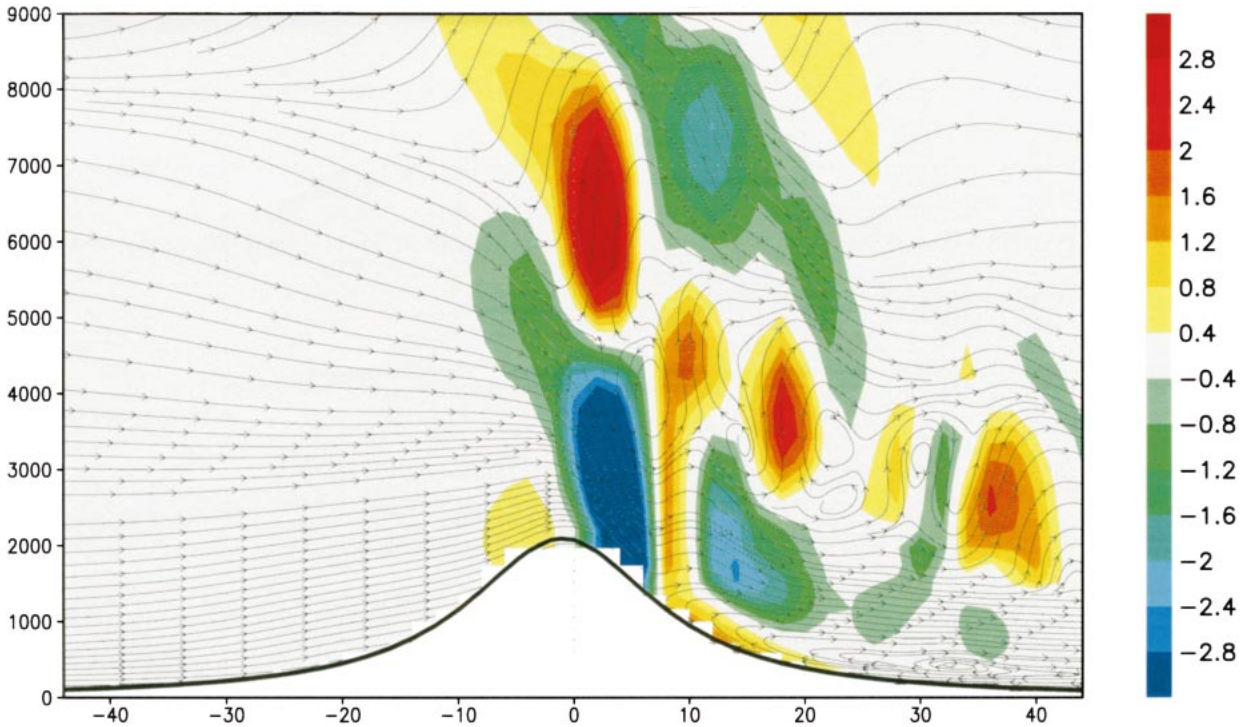

FIG. 5. As Fig. 4 but after 2 h.

$$D = \delta_x F_z u + \delta_z F_x w \quad \text{and} \tag{18}$$

$$\frac{\partial T}{\partial t} = -\overline{F_z u \delta_x T}^{x} - \overline{F_x w \delta_z T}^{z} - \frac{p}{\rho C_v} D. \tag{19}$$

Time integration is done using the three-time-level Klemp and Wilhelmson (1978) scheme, in the same way as used by Dudhia (1993) or Steppeler et al. (2002). The advection terms in Eqs. (15)–(19) are treated by the leapfrog time discretization. The other terms, corresponding to the fast waves, are treated using a smaller time step, corresponding to the CFL criterion for sound waves. The tendency obtained from advection is kept fixed when doing the small time steps. The time integration of the fast waves is done using the foreward–backward scheme, with implicit treatment of terms corresponding to the vertical discretization. When an averaging operator is taken for a grid point where one of the points is under the mountain, the average is taken to be the value at the grid point outside the mountain. For example if for the term $\overline{F_z u \delta_x T}^{x}$ from Eq. (19) $u_{i+1/2,k}$ is under the mountain, $F_z u_{i+1/2,k} \delta_x T$ is defined to be $F_z u_{i-1/2,k} \delta_x T$.

3. Results

According to Gallus and Klemp (2000), a step-mountain realization of the lower boundary does not properly represent the solution corresponding to a smooth mountain, in particular for the hydrostatic mountain wave. This solution is well captured by terrain-following coordinate models. In order to see if the method proposed here has problems of this kind, two tests proposed by Gallus and Klemp (2000) have been performed. A bell-shaped mountain of height 400 m and half-width 1000 m is used. The topographic height $h(x)$ is assumed to be

$$h(x) = \frac{h_0}{1 + (x/a)^2}. \tag{20}$$

Model runs have been performed with a horizontal resolution of 2 km and 49 vertical layers, the layers increasing from 100 to 400 m with increasing z. The computations were done on a 3000×49 grid. This rather large grid was used to absorb the shock waves when the high mountain of 2100 m was used. Lower mountains in two dimensions could be simulated with a smaller grid. The initial horizontal velocity was $u_0 = 10$ m s^{-1}.

Figure 2 shows the field w after a run time of 2.5 h for the shaved elements and the terrain-following coordinates. The height of the mountain is $h_0 = 400$ m. No problems of the kind Gallus and Klemp reported can be seen. Figure 3 shows the horizontal wind velocity u at the same forecast time. The excessive wind shadow reported by Gallus and Klemp (2000) is not present. Both Figs. 3a and 3b are rather similar. As a stability test, computations using a mountain height of 2100 m have also been performed. For these tests the rather large computational area that was introduced was useful. In the beginning of the forecast this rather high mountain produced shock waves that had to be removed by a proper treatment of the lateral boundaries. Figure 4 shows streamlines and the vertical velocity field after $t = 4$ h. As the Froude number is larger than 1, the flow is no longer stationary. After a system of gravitational waves forms in the beginning, some nonstationary vortex shedding occurs. The flow is strongly variable in time, as can be seen by a comparison with the field at 2 h, given in Fig. 5. The physical interpretation of these effects is difficult, as the model does not have a physical diffusion, but rather a numerical fourth-order diffusion operator is used.

4. Conclusions

Approximations for z-coordinate nonhydrostatic atmospheric models were derived based on the shaved-element finite-volume method using the thin-wall approximation. The finite-difference equations are centered-difference equations for those elements that are not cut by the topographic function. For the elements cut by the topographic function the finite-difference equations can be formulated using flux limiters in the horizontal and vertical directions. The model was derived here on the C grid and the solutions near a bell-shaped smooth mountain were rather similar to those obtained by a terrain-following version of the model.

Acknowledgments. Financial support was granted by CIRM-ITC and DWD for visits or JS to Trento and LB to Offenbach, which is gratefully acknowledged. The authors thank J. Klemp, G. Doms, U. Schättler, and G. Rosatti for helpful discussions.

REFERENCES

Adcroft, A., C. Hill, and J. Marshall, 1997: Representation of topography by shaved cells in a height coordinate ocean model. *Mon. Wea. Rev.,* **125,** 2293–2315.

Bonaventura, L., 2000: A semi-implicit, semi-Lagrangian scheme using the height coordinate for a nonhydrostatic and fully elastic model of atmospheric flows. *J. Comput. Phys.,* **158,** 186–213.

Dudhia, J., 1993: A nonhydrostatic version of the Penn State–NCAR Mesoscale Model: Validation tests. *Mon. Wea. Rev.,* **121,** 1493–1513.

Gallus, W., and J. Klemp, 2000: Behavior of flow over step orography. *Mon. Wea. Rev.,* **128,** 1153–1164.

Klemp, J., and R. Wilhelmson, 1978: The simulation of three-dimensional convective storm dynamics. *J. Atmos. Sci.,* **35,** 1070–1096.

Mesinger, F., Z. Janjic, S. Nickovic, D. Gavrilov, and D. Deaven, 1988: The step-mountain coordinate: Model description and performance for cases of alpine lee cyclogenesis and for a case of an Appalachian redevelopment. *Mon. Wea. Rev.,* **116,** 1493–1518.

Saito, K., G. Doms, U. Schaettler, and J. Steppeler, 1998: 3-D mountain waves by the Local Modell of DWD and the MRI Mesoscale Nonhydrostatic Model. *Meteor. Geophys.,* **49,** 7–19.

——, J. Steppeler, T. Kato, Eito, and A. N. Murata, 2001: Report on the Third International SRNWP (Short-Range Numerical Weather Prediction) Workshop on Nonhydrostatic Modelling. *Bull. Amer. Meteor. Soc.,* **82,** 2245–2250.

Steppeler, J., 1982: Treatment of discontinuous finite element basis functions as distributions. *Beitr. Phys. Atmos.,* **55,** 43–60.
——, G. Doms, U. Schättler, H. W. Bitzer, A. Gassmann, U. Damrath, and G. Gregoric, 2002: Meso gamma scale forecasts by the nonhydrostatic models LM. *Meteor. Atmos. Phys.,* in press.
Sundqvist, H., 1976: On vertical interpolation and truncation in connection with use of sigma system models. *Atmosphere,* **14,** 37–52.
Thomas, S., C. Girard, G. Doms, and U. Schättler, 2000: Semi-implicit scheme for the DWD Lokal-Modell. *Meteor. Atmos. Phys.,* **73,** 105–125.